Diagn Interv Radiol 2017; 23:300–306

HEAD AND NECK IMAGING

ORIGINAL ARTICLE

Accuracy of turbo spin-echo diffusion-weighted imaging signal intensity measurements for the diagnosis of cholesteatoma

Burçe Özgen
Elif Bulut
Anıl Dolgun
Munir Demir Bajin
Levent Sennaroğlu

PURPOSE
We aimed to evaluate the diagnostic accuracy of turbo spin-echo diffusion-weighted imaging (TSE-DWI) at 3 T, for cholesteatoma (CS) diagnosis, using qualitative and quantitative methods with numerical assessment of signal intensity (SI), signal intensity ratios (SIR), and apparent diffusion coefficient (ADC) values.

METHODS
In this retrospective study, two blinded observers independently evaluated the preoperative TSE-DWI images of 57 patients who were imaged with a presumed diagnosis of CS. Qualitative assessment with respect to the SI of the adjacent cortex and quantitative measurements of SI, SIR, and ADC values were performed.

RESULTS
Surgery with histopathologic examination revealed 30 CS patients and 27 patients with non-cholesteatoma (NCS) lesions including chronic inflammation and cholesterol granuloma. On TSE-DWI, 96.7% of the CS lesions and none of the NCS lesions appeared hyperintense compared with the cortex. The mean SI and SIR indices of the CS group were significantly higher and the mean ADC values significantly lower compared with those of the NCS group ($P < 0.001$). Using specific cutoff values for SI (92.5) and SIR (0.9), CS could be diagnosed with 100% sensitivity and specificity. The use of quantitative imaging further increased the sensitivity of the TSE-DWI technique.

CONCLUSION
The quantitative indices of SI, SIR, and ADC of TSE-DWI appear to be highly accurate parameters that can be used to confirm the diagnosis of CS.

Cholesteatomas (CS) are enlarging collections of keratin within a sac of squamous epithelium within the middle ear cavity, which can result in hearing loss and may also lead to severe complications such as intracranial abscess, meningitis, and facial paralysis (1, 2). Although the aim of the treatment is complete surgical excision, recurrence is a common problem (3). Currently, with the implementation of non-echoplanar diffusion-weighted imaging (DWI), low-yield, traditional second-look procedures are no longer necessary for patients who are at low risk of developing recurrences (4, 5). The high signal intensity of the CS in diffusion-weighted images has a high reported diagnostic accuracy (6–9). However, other lesions of the middle ear such as chronic inflammatory tissue, abscess, cholesterol granuloma, and iatrogenic material such as impacted fat material or bone powder from previous surgery can also result in a relatively high DWI signal, resulting in false positive results (7, 10–14). It is therefore important to determine an objective and reliable method in the assessment of DWI in order to correctly diagnose initial, residual, or recurrent CS. This study was designed to establish the value of qualitative, as well as quantitative parameters including signal intensity (SI), signal intensity ratio (SIR), and apparent diffusion coefficient (ADC) values for the diagnosis of CS using turbo spin-echo (TSE)-DWI at 3 Tesla (T).

From the Departments of Radiology (B.Ö. ✉ *burce@hacettepe.edu.tr*, E.B.), Biostatistics (A.D.) and Otolaryngology (M.D.B., L.S.), Hacettepe University School of Medicine, Ankara, Turkey.

Received 24 January 2017; revision requested 9 March 2017; last revision received 14 March 2017; accepted 22 March 2017.

Published online 4 May 2017.
DOI 10.5152/dir.2017.16024

You may cite this article as: Özgen B, Bulut E, Dolgun A, Bajin MD, Sennaroğlu L. Accuracy of turbo spin-echo diffusion-weighted imaging signal intensity measurements for the diagnosis of cholesteatoma. Diagn Interv Radiol 2017; 23:300–306.

Methods

Patient selection

This was a retrospective study undertaken at a single academic setting. A database search was initially performed to identify all patients who had undergone 3 T magnetic resonance imaging (MRI) of the temporal bone with TSE-DWI for the evaluation of cholesteatoma between March 2014 and March 2016. Only the data of patients who had subsequently undergone surgery were included in the study. Fifty-seven patients who met these criteria were identified. Surgical notes and histopathologic results were available for all patients.

The study was approved by the Institutional Ethics Board (GO 15/598-12) and adhered to the tenets of the Declaration of Helsinki. Informed consent was not obtained as the data was collected retrospectively and all imaging data were anonymized.

Imaging technique

MRI examinations were performed with a 3 T MRI scanner (Ingenia, Philips) using a standard eight-channel head coil. The standard temporal bone protocol for cholesteatoma evaluation included transverse T1-weighted imaging, transverse and coronal T2-weighted imaging, and coronal TSE-DWI without contrast injection. The TSE-DWI was obtained in the coronal plane with the following parameters: repetition time (TR)/echo time (TE), 6200/67 ms; 3 mm slice thickness without gap; number of excitation (NEX), 4; matrix, 124×88; field of view (FOV), 220×180. Two b values were obtained (b=0 and b=1000). The ADC maps were automatically generated on the scanner and transferred to the PACS archive. Axial T1-weighted imaging was performed with a TR/TE, 475/12 ms; flip angle, 90; NEX, 1; 2 mm slice thickness, FOV, 180×180 mm; matrix, 704×704. Axial TSE T2-weighted imaging was obtained with TR/TE, 3000/80; flip angle, 90; NEX, 2; slice thickness, 2 mm; FOV, 180×180 mm; matrix, 640×640. Coronal TSE T2-weighted imaging was obtained with TR/TE, 3000/80; flip angle, 90; NEX, 2; slice thickness, 2 mm; FOV, 168×168 mm; matrix, 640×640.

Main points

- Turbo spin-echo diffusion-weighted imaging is highly accurate for diagnosing cholesteatoma using a 3 T magnet.
- Diffusion-weighted signal intensity (SI), signal intensity ratio (SIR), and apparent diffusion coefficient are highly accurate parameters for the diagnosis of cholesteatoma.
- SI and SIR had 100% accuracy for cholesteatoma diagnosis at specific cutoff values.
- The quantitative techniques further increase the accuracy of the qualitative method.

Imaging evaluation

Two radiologists, who were blinded to the histopathologic results, independently evaluated the images of the patients in a random order. The maximum dimension of signal abnormality was measured on images obtained by TSE-DWI for each patient.

The corresponding signal properties of the lesions were assessed on T1-weighted images; their appearance (homogenous vs. heterogeneous) and their signal intensity with respect to the adjacent temporal cortex were noted.

Qualitative assessment of DWI included comparison of the lesion SI in the trace images with that of the adjacent inferior temporal cortex. The comparisons were classified as hyperintense, isointense, or hypointense.

Region-of-interest (ROI) measurements were then performed on the lesions both in trace diffusion-weighted images and in the ADC maps. The SI measurements were obtained with a standard sized ROI (3 mm^2) that was placed within the brightest part of signal abnormality on the trace images. The mean (SI) and maximum (SI_{max}) SI values on the trace images were recorded from that single ROI for each patient (Fig. 1). Mean SI measurements from the inferior temporal cortex (SI_T) were also obtained for qualitative comparisons with the lesion, as well as for calculation of SIR, which was calculated based on SI of the lesion using the following formulas: $SIR = SI/SI_T$, $SIR_{max} = SI_{max}/SI_T$.

The ADC value of the lesion was recorded by manual outlining of a same-size 3 mm^2 uniform ROI within the lesion. The location of ROI was determined with the use of a cross-match on trace images. The mean ADC values were recorded for each patient. Additionally, ADC values from the pons (ADC_p) were also obtained in order to compare the ADC_p values in different subgroups as an internal quality check as well as for a comparison with the known ADC values in the literature.

The observers noted the presence/absence of image distortion from susceptibility artifacts on the diffusion-weighted images and particularly on the ADC maps. None of the cases had artifacts involving the areas where the ROIs were placed and therefore the artifacts did not preclude the measurements of the ADC values. Both observers performed all measurements, separately and independently for the assessment of interobserver agreement. However, the diagnostic value of TSE-DWI was assessed through the measurements of the more experienced observer.

Statistical analysis

Statistical analysis was performed using SPSS software, version 21.0 (IBM Corp.). Numerical data were reported as mean ± standard deviation and categorical data as frequency and percentage. The Student's t-test and Chi-square test were performed to compare the differences of age and gender between CS and non-cholesteatoma (NCS) groups. Differences in SI, SIR, mean and maximum ADC values between groups were evaluated using the Mann-Whitney U test. Receiver operating characteristic (ROC) analyses were further used to evaluate the diagnostic value of the significant parameters in discriminating CS from NCS lesion. The optimum cutoff value for prediction of CS was determined for different parameters, to give the optimum combination of sensitivity and specificity. Interobserver agreements between the two radiologists' measurements were assessed using Pearson correlation coefficient. A P value of < 0.05 was defined as statistically significant.

Results

Fifty-seven MRI studies with TSE-DWI were evaluated. The subjects consisted of 29 males and 28 females with an age range of 5–60 years (mean, 37.6±16.2 years). Twenty-six patients had no prior surgery and 31 patients were postoperative cases who had undergone prior surgery for CS. The patient data and surgical/histopathologic results are summarized in Table 1.

The patients were divided according to postoperative pathologic findings into CS and NCS groups. There were 30 patients with the surgical and histopathologic diagnosis of CS. The NCS group (n=27) included patients with histopathologic diagnosis of chronic granulation tissue and/or inflammation (n=24), cholesterol granuloma of the middle ear (n=2), and middle ear adenoma (n=1). For the NCS patients the deci-

Table 1. Descriptive data of study patients

	Cholesteatoma (n=30)	Non-cholesteatoma (n=27)	*P*
Age (years), mean±SD (range)	36.2±16.0 (5–60)	39.1±16.6 (12–61)	0.477
Sex, n	12 F, 18 M	16 F, 11 M	0.146
Prior history of surgery, n/N (%)	17/30 (56.7)	14/27 (51.9)	0.716

SD, standard deviation; F, female; M, male.

Table 2. Mean values of SI, SIR, and ADC values in cholesteatoma and non-cholesteatoma lesions

	Cholesteatoma (n=30)	Non-cholesteatoma (n=27)	*P*
SI	133.1±24.1 (93–187)	49.1±14.9 (26–92)	<0.001
SI_{max}	171.9±32.2 (113–249)	60.6±18.4 (29–110)	<0.001
SI_T	95.4±10.0 (75–116)	92.4±10.1 (73–115)	0.317
SIR	1.4±0.3 (0.9–1.9)	0.5±0.1 (0.3–0.9)	<0.001
SIR_{max}	1.8±0.3 (1.0–2.6)	0.7±0.2 (0.3–1.1)	<0.001
Mean ADC ($\times 10^{-3}$ mm^2/s)	1.0±0.1 (0.7–1.3)	2.1±0.6 (0.9–2.8)	<0.001
ADC_p ($\times 10^{-3}$ mm^2/s)	1.1±0.7 (1.0–1.3)	1.1±0.9 (0.90–1.3)	0.497

The values are given as mean ± standard deviation (range).
SI, mean signal intensity; SI_{max}, maximum signal intensity; SI_T, mean signal intensity measured from the inferior temporal cortex; SIR, signal intensity ratio; ADC, apparent diffusion coefficient; ADC_p, ADC value of the pons.

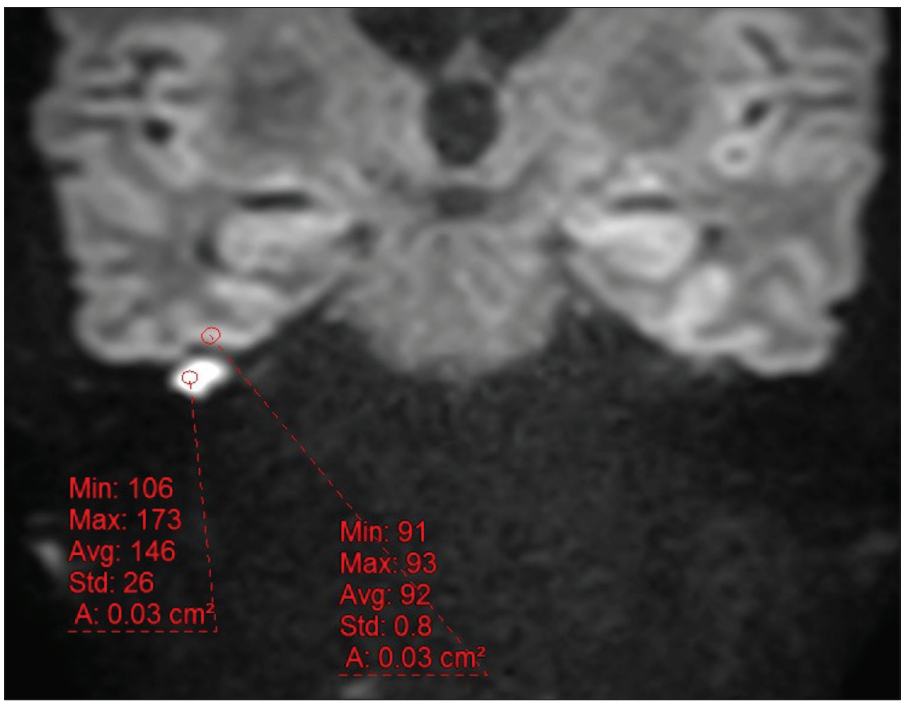

Figure 1. Region-of-interest (ROI) placement and signal intensity (SI) measurements. Coronal turbo spin-echo diffusion-weighted imaging (TSE-DWI) of a patient with the histopathologic diagnosis of cholesteatoma demonstrating the high signal of the cholesteatoma lesion. A standard sized ROI (3 mm^2) was placed on the lesion and the mean and maximum SI (SI and SI_{max}) were recorded. Additionally, the mean SI of the adjacent inferior temporal cortex was recorded (SI_T).

sion for the surgery had been made based on the MRI findings (in cases of cholesterol granuloma, middle ear adenoma) or for hearing restoration such as staged ossicular chain reconstruction (for patients with chronic inflammation).

Of the 30 CS patients, 12 were female and 18 male, with a mean age of 36.2±16 years (range, 5–60 years). Of the 27 NCS patients, 16 were female and 11 male, with a mean age of 39.1±16.6 years (range, 12–61 years). There were no statistically significant differences between CS and NCS patients with respect to age and sex ($P = 0.477$ and $P = 0.146$, respectively). The ratio of patients with prior surgery was similar in both groups (n=17 in CS group, n=14 in NCS group; $P = 0.716$).

The average largest size of the CS lesions was 9.2±5.8 mm (range, 4.0–30.0 mm). Of 30 CS patients, 21 (70%) had lesions measuring less than 1 cm in their maximum diameter.

The T1 signal of the lesions in the CS group was isointense or hypointense to the brain parenchyma in 28 cases (93.3%). Two cases (6.7%) had mixed hypo/isointense and hyperintense signals on T1-weighted imaging. However, upon correlation with the DWI, the hyperintense regions were noted to correspond to areas outside the zone of high diffusion signal, likely representing chronic inflammatory tissue accompanying the CS lesions. Indeed, in one of those cases, surgical notes confirmed the presence of inflammation and purulent material in the middle ear cavity adjacent to the CS. In the NCS group, two cases with the histopathologic diagnosis of cholesterol granuloma (7.4%) were hyperintense on T1-weighted imaging as expected. However, seven cases with the diagnosis of chronic granulation tissue/inflammation (25.9%) also had high T1 signal compared with brain parenchyma. Six additional cases with chronic granulation tissue/inflammation diagnosis (22.2%) and the case with middle ear adenoma had mixed signal intensities with hyperintense and hypointense regions. Eleven remaining cases with chronic inflammation diagnosis (40.7% of all NCS cases) had hypointense T1 signal.

In the CS group, 29 lesions (96.7%) had higher intensities compared with cortex on TSE-DWI (Fig. 2), but one patient with CS had a lesion that was isointense with cortex. In the NCS group, 20 patients (74%) had lesions with lower signal compared with cortex, while seven patients (26%) had lesions isointense to cortex (Figs. 3, 4). The hyperintensity of a lesion compared with the cortex was suggestive of CS with 96.7% sensitivity, 100% specificity, 100% positive predictive value (PPV), and 96.4% negative predictive value (NPV). The hyperintensity on trace TSE-DWI compared with cortex was diagnostic of a CS with an accuracy of 98.25%.

The results of the quantitative assessment of SI and SIR differences of the CS and NCS groups are detailed in Table 2. There was no statistically significant difference between

the mean SI of the temporal cortex of the CS and NCS groups (P = 0.317). However, the mean SI of the CS lesion itself was significantly higher than the mean DW signal of lesions identified as NCS (P < 0.001). Using a cutoff value of ≥92.5 for the mean SI, the TSE-DWI was diagnostic of CS with a sensitivity and specificity of 100%. Similarly, using a maximum SI cutoff value of ≥111.5, the diagnosis of CS could be made with a sensitivity and specificity of 100%. The diagnostic performance of different quantitative measurements are detailed in Table 3 and the comparison of different SI measurement types are illustrated with Boxplots in Fig. 5.

The mean SIR and mean SIR_{max} were higher in CS group than in NCS group and this difference was statistically significant (P < 0.001) for both measurements. For a cutoff value of mean SIR ≥0.9, TSE-DWI was diagnostic for CS with a sensitivity and specificity of 100%. If the maximum SIR was used with a cutoff value of 1.06, the diagnosis of CS could again be made with a sensitivity and specificity of 100%.

The mean ADC values were 1.0±0.1 $\times 10^{-3}$ mm^2/s for the CS group and 2.0±0.6 $\times 10^{-3}$ mm^2/s for the NCS group. The mean ADC_p was 1.1±0.8 $\times 10^{-3}$ mm^2/s for CS group and 1.1±0.9 $\times 10^{-3}$ mm^2/s for the NCS group. There was no statistically significant difference in the mean ADC_p values between the two groups (P = 0.497). However, the mean ADC value of CS was significantly lower than the ADC values of NCS (P < 0.001). A lesion with an ADC value ≤1.24 $\times 10^{-3}$ mm^2/s could be diagnosed as CS with 96.7% sensitivity, 88.9% specificity, 90.6% PPV, and 96% NPV. The diagnostic value of different types of techniques and parameters of measurements are summarized in Table 3. The comparison of the quantitative indices in CS and NCS patients are illustrated with Boxplots in Fig. 5.

There was a strong interobserver correlation for the SI and ADC measurements performed by two observers using the Pearson correlation coefficient (r=0.94 for SI and r=0.97 for ADC, P < 0.001).

Table 3. Diagnostic performance of different quantitative measurements for the diagnosis of cholesteatoma

	Cutoff value	Sensitivity (%)	Specificity (%)	PPV (%)	NPV (%)	Accuracy
SI	>92.5	100	100	100	100	100
SI_{max}	>111.5	100	100	100	100	100
ADC ($\times 10^{-3}$ mm^2/s)	<1.2×10^{-3}	97	89	90	96	93
SIR	>0.9	100	100	100	100	100
SIR_{max}	>1.1	100	100	100	100	100

PPV, positive predictive value; NPV, negative predictive value; SI, mean signal intensity; SI_{max}, maximum signal intensity; ADC, apparent diffusion coefficient; SIR, signal intensity ratio; SIR_{max}, maximum signal intensity ratio.

Discussion

In the last decade, DWI has proved its value for initial and follow-up evaluation of middle ear CS and currently non-echoplanar DWI has replaced the second look surgery for the follow-up evaluation of postoperative patients in many centers (11, 13, 15). Several different non-echoplanar based techniques have been developed by different vendors, including half-Fourier acquisition single-shot turbo spin-echo (HASTE) DWI and periodically rotated overlapping parallel lines with enhanced reconstruction (PROPELLER) DWI (13, 16–19). TSE acquisition can be made sensitive to diffusion by using a gradient before and after the 180° refocusing pulse, a method known as the Alsop method for diffusion TSE (20). TSE-based diffusion can also be very useful in areas such as skull base and temporal bone, since TSE sequences are inherently less sensitive to susceptibility differences (21). In our study, we evaluated the value of specific qualitative as well as quantitative assessments to increase the accuracy of the TSE-DWI technique.

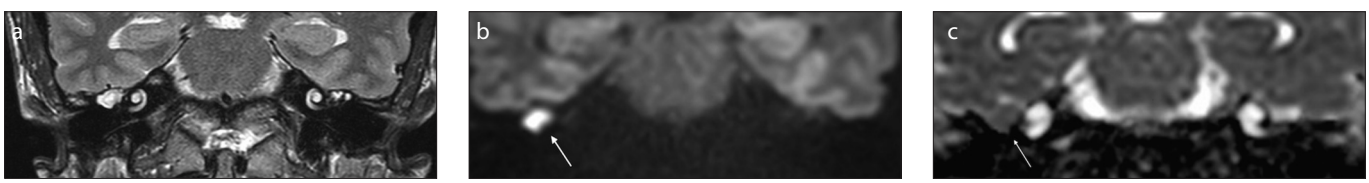

Figure 2. a–c. Coronal T2-weighted imaging **(a)**, coronal TSE-DWI **(b)**, and corresponding apparent diffusion coefficient (ADC) map **(c)** of a patient with the histopathologic diagnosis of cholesteatoma, revealing a high T2 signal lesion **(a)**, with increased signal on DWI (**b,** *arrow*). The lesion is hyperintense compared with the adjacent brain parenchyma and shows corresponding low ADC signal on the ADC map (**c,** *arrow*).

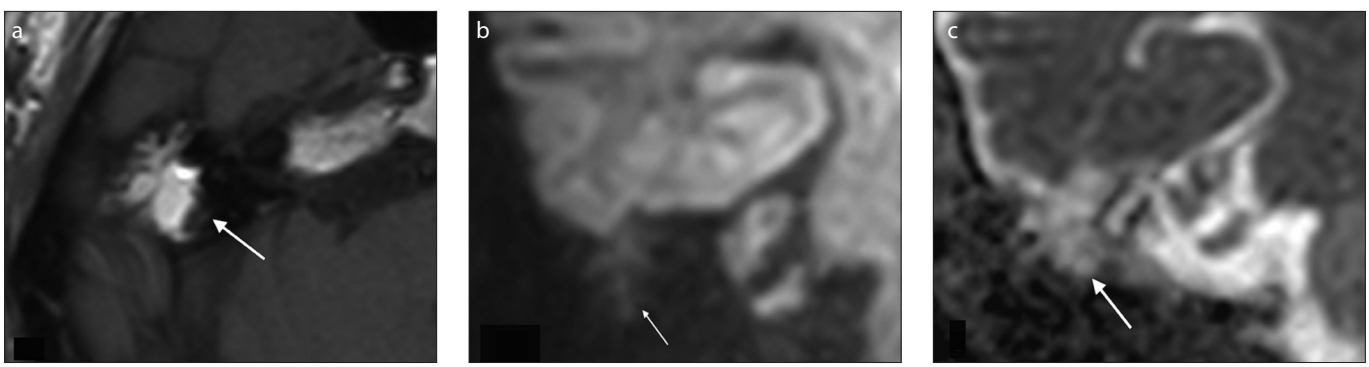

Figure 3. a–c. A patient with the histopathologic diagnosis of cholesterol granuloma. Axial T1-weighted image **(a)** shows a T1 hyperintense lesion *(arrow)*. TSE diffusion-weighted image **(b)** shows subtle increase in signal, with the ADC map **(c)** showing correspondingly increased signal.

With the routine qualitative assessment, using visual comparison of the signal intensity to the adjacent temporal cortex, the accuracy of the TSE-DWI for the diagnosis of CS was very high, with 96.7% sensitivity and 100% specificity. These results are similar to previously published qualitative studies in the literature reporting 100% sensitivity and specificity (22–25). However, most qualitative non-echoplanar DWI studies in the literature have reported slightly lower sensitivity (82%–92%) and specificity (86%–96%) values (5, 6, 14, 19, 26–28). The false-negative cases and thus the relatively lower sensitivity levels for the non-echoplanar evaluation of CS are reported to be due to the insufficiency of the technique to demonstrate mural and very small lesions (17, 19, 22). The lesions in our study were of moderate size (mean, 9.2±5.81 mm) with a few large lesions. The smallest lesion in our series was 4 mm in its largest dimension. Mural CSs are dry retraction pockets that have auto-evacuated their contents and as the pocket has lost its keratin, the DWI fails to detect the residual surrounding epithelium that has a persistent aggressive potential (13, 22). These lesions are known to cause false negative results on DWI; however, none of our patients had a mural CS. The relatively high accuracy level obtained in the current study may be attributed to the paucity of small sized lesions in our series. However, these results may also be partly due to increased signal acquisition in a 3 T magnet. Further studies with smaller sized lesions, comparing the TSE-DWI sequence in magnets of different field strength might elucidate the cause of the observed differences in sensitivity.

The main DWI diagnostic CS criterion is lesion hyperintensity on high b value images assessed qualitatively (15, 29). Although the qualitative non-echoplanar methods have high diagnostic accuracy (as seen above), there are still instances where the high signal of diffusion-weighted images does not unequivocally represent CS. The false positive cases reported in the literature include cholesterol granuloma, abscess, inserted fat graft, bony cement as well as chronic inflammatory tissue (7, 10–14, 30). The cholesterol granuloma can be differentiated by its T1 hyperintensity, while the abscess can be differentiated by its acute clinical presentation as well as its very low ADC value (10, 12, 18). The surgical material that may result in a high DWI signal can be diagnosed with appropriate clinical history. However, chronic inflammatory tissue is difficult to differentiate from CS on clinical grounds. These lesions are quite common in the same patient pop-

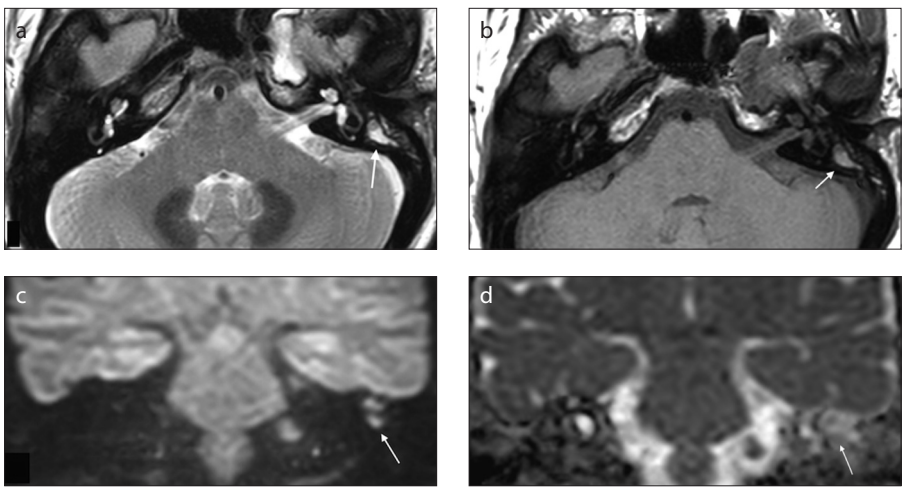

Figure 4. a–d. A 45-year-old woman with chronic middle ear inflammation and granulation tissue. Axial T2-weighted image **(a)** shows a high T2 signal lesion *(arrow)*, with mild signal increase compared with the brain parenchyma on axial T1-weighted image **(b)**. The lesion demonstrates high signal on DWI **(c)** but is isointense compared with the temporal cortex and has mixed signal on the ADC map **(d)**.

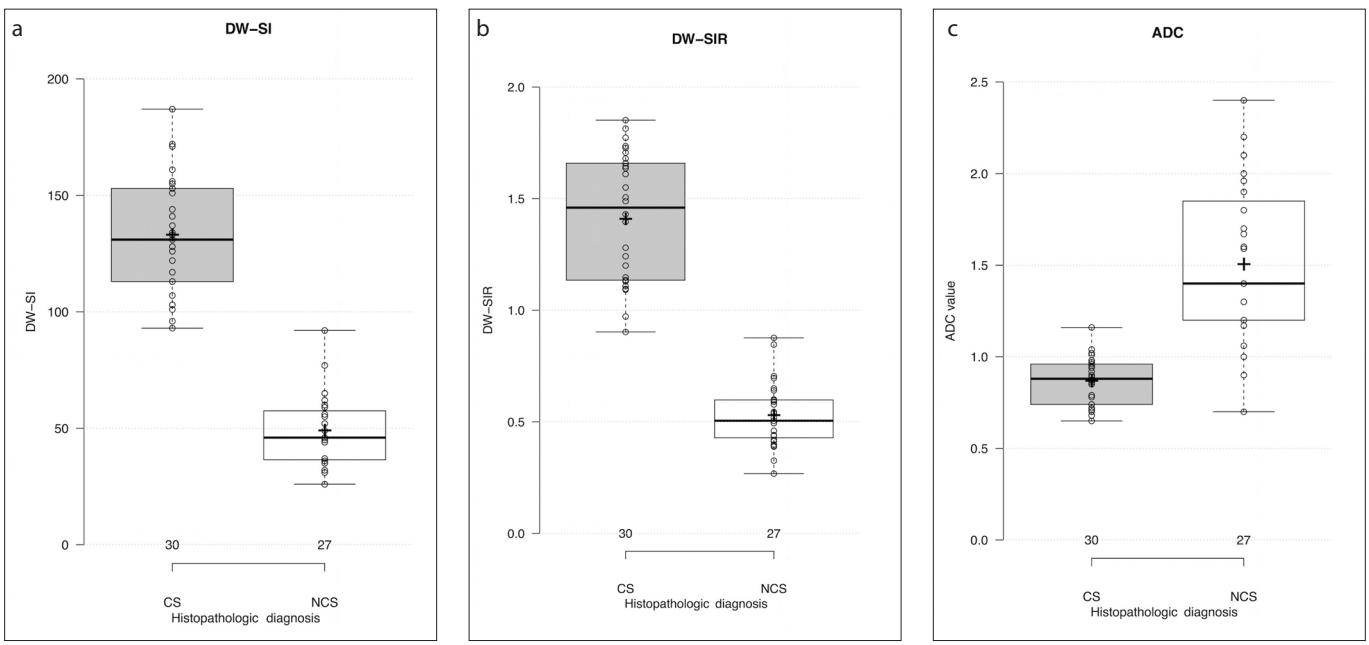

Figure 5. a–c. Comparison of mean signal intensity (SI) **(a)**, signal intensity ratio (SIR) **(b)**, and ADC values **(c)** in cholesteatoma (CS) and non-cholesteatoma (NCS) patients. Boxplots showing the distribution of SI, SIR, and ADC values. Center lines show the medians; box limits indicate the 25th and 75th percentiles as determined by R software; whiskers extend to minimum and maximum values; crosses represent sample means; data points are plotted as open circles.

ulation group as illustrated in our NCS cases; inflammatory lesions constituted the majority (88.9%) of our NCS group. In general, middle ear inflammation has a hypointense DWI signal compared with the brain parenchyma on DWI. Still, certain inflammatory lesions, which are isointense to the cortex, may demonstrate relatively brighter signal on non-echoplanar images and may result in a false positive interpretation (14, 21). The presence of six cases in this study with such imaging characteristics supports this notion. On the other hand, CS may also have a relatively isointense signal compared with the cortex as reported by Lingam et al. (14), resulting in false negative results. In this study, we aimed to assess whether the quantitative analysis with SI/SIR and ADC values could be used to increase the sensitivity of the TSE-DWI method (12, 14, 31). A previous study with numerical assessment of SI on BLADE-DWI reported significant differences between the mean SIR of 3.28–3.75 in CS compared with a mean SIR of NCS lesions of 2.38; however, the sensitivity of this SIR measurement and the cutoff value was not reported in that study (31). The current study confirms these prior observations using a larger patient population, as well as evaluating the accuracy of these parameters with specific cutoff values (92.5 for SI and 0.9 for SIR measurements). Furthermore, we were able to correctly identify a CS case with isointense imaging characteristics as well as seven NCS cases that were isointense to the cortex and difficult to characterize with qualitative assessment only; thus, the quantitative measurements were able to further increase the accuracy of the qualitative non-echoplanar technique.

We also wanted to assess whether there were differences in SI and SIR values when a maximum as opposed to mean SI value was used to identify CS form NCS lesions. The accuracy of maximum SI and maximum SIR were found to be similar to that obtained with mean SI and SIR values, therefore either the mean or the maximum value can be used to make a quantitative assessment.

The ADC values have been used to differentiate CS from abscess as the latter has a much lower ADC value (0.4–0.6$\times10^{-3}$ mm^2/s) than CS (0.8–1.1 $\times10^{-3}$ mm^2/s) (12, 15); however, to our knowledge a cutoff value has not been determined to separate CS from other inflammatory lesions that constituted the majority (24 out of 27) of our NCS group. Dremmen et al. (7) mentioned that in their series the ADC value was not helpful for their false positive cases. On the other hand, Lingam et al. (14) determined a cutoff value to differentiate CS from NCS lesions with 100% sensitivity and 96% specificity; however, they did not report the final histopathologic diagnosis of their NCS group. In our series, the ADC values were significantly different between NCS and the CS lesions. Specifically, when an ADC value of 1.24 $\times10^{-3}$ mm^2/s was used as a cutoff value, this parameter had good sensitivity and specificity for the differentiation of CS from NCS lesions. It is interesting to note that the cutoff value of 1.24 $\times10^{-3}$ mm^2/s calculated from our data is similar to the previously calculated cutoff value of 1.3 $\times10^{-3}$ mm^2/s by Lingam et al. (14). Our sensitivity and specificity values for that particular cutoff ADC value were slightly lower than the ones reported previously (14). This may partly be due to the fact that we performed a single measurement on a single slice compared with multiple measurements performed on multiple slices in the above-mentioned study.

It is also interesting to note that the mean ADC value for CS in this study (1.0±0.1 $\times10^{-3}$mm^2/s) was higher than the previously reported mean ADC values (0.7–0.9 $\times10^{-3}$ mm^2/s) (12, 14, 18). The difference may be due different DWI techniques used and in particular due to parallel imaging techniques used in 3 T TSE-DWI. The aliased images used for image reconstruction in parallel imaging may result in unfolding artifacts causing variation in the ADC values (32). The mean ADC of the pons (1.12–1.14 $\times10^{-3}$ mm^2/s) calculated in our study was also higher than the mean ADC value established for pons (0.7 $\times10^{-3}$ mm^2). It has been previously reported that non-echoplanar DWI techniques yield different ADC values than echoplanar techniques (33).

The SI measurements are not usually performed for lesion characterization as the MRI has intensity variations from magnetic field inhomogeneity and scanner-related artifacts, making it impossible to generate a standardized, sequence-specific intensity scale. We thus performed and reported the SIR calculations to normalize signal differences. Nevertheless, our SI measurements were repeatable (as demonstrated by strong correlation among the observers) and there was no difference in accuracy between the SI and SIR measurements. There was no significant difference between the mean SI of the temporal cortex of the CS and NCS groups (P = 0.317) confirming the validity of our measurements. As the signal intensity of a given lesion depends not only on the tissue but also on the instrument parameters, there is no way to determine the validity of the presented mean SI measurements and calculated cutoff values, other than to measure the reproducibility of these results in other scanners with similar strengths. It may be advisable for each center to determine their specific threshold values for further assessment.

Our study has several limitations. First, the assessment was performed using a sequence from a specific vendor. The results would need to be repeated and verified with different non-echoplanar sequences in different field strengths. As it was the case with previous studies, there was a selection bias as most patients with negative DWI results do not undergo explorative tympanostomy. Additionally the lack of small lesions in our series as well as absence of patients with bone grafts or silicon implants were other limiting features. Yet, despite these limitations, it is our opinion that the current study contributes to the diagnostic management of CS lesions by proposing highly accurate quantitative and qualitative DWI parameters.

In conclusion, we found TSE-DWI to be highly accurate for diagnosing CS using a 3 T magnet. Our study showed that qualitative and quantitative measurements using SI and SIR have high sensitivity and specificity with a high degree of interobserver agreement. The use of quantitative imaging further increased the sensitivity of this non-echoplanar technique. Therefore, utilization of SI, SIR, and ADC parameters at specific cutoff values is recommended for the diagnosis of CS and improved clinical care.

Conflict of interest disclosure

The authors declared no conflicts of interest.

References

1. Friedmann I. Epidermoid cholesteatoma and cholesterol granuloma; experimental and human. Ann Otol Rhinol Laryngol 1959; 68:57–79. [CrossRef]
2. Semaan MT, Megerian CA. The pathophysiology of cholesteatoma. Otolaryngol Clin North Am 2006; 39:1143–1159. [CrossRef]
3. Neudert M, Lailach S, Lasurashvili N, Kemper M, Beleites T, Zahnert T. Cholesteatoma recidivism: comparison of three different surgical techniques. Otol Neurotol 2014; 35:1801–1808. [CrossRef]
4. Keeler JA, Kaylie DM. Cholesteatoma: Is a second stage necessary? Laryngoscope 2016; 126:1499–1500. [CrossRef]
5. Jindal M, Riskalla A, Jiang D, Connor S, O'Connor AF. A systematic review of diffusion-weighted magnetic resonance imaging in the assessment of postoperative cholesteatoma. Otol Neurotol 2011; 32:1243–1249. [CrossRef]

6. van Egmond SL, Stegeman I, Grolman W, Aarts MC. A systematic review of non-echo planar diffusion-weighted magnetic resonance imaging for detection of primary and postoperative cholesteatoma. Otolaryngol Head Neck Surg 2016; 154:233–240. [CrossRef]
7. Dremmen MH, Hofman PA, Hof JR, Stokroos RJ, Postma AA. The diagnostic accuracy of non-echo-planar diffusion-weighted imaging in the detection of residual and/or recurrent cholesteatoma of the temporal bone. AJNR Am J Neuroradiol 2012; 33:439–444. [CrossRef]
8. Li PM, Linos E, Gurgel RK, Fischbein NJ, Blevins NH. Evaluating the utility of non-echo-planar diffusion-weighted imaging in the preoperative evaluation of cholesteatoma: a meta-analysis. Laryngoscope 2013; 123:1247–1250. [CrossRef]
9. Lingam RK, Nash R, Majithia A, Kalan A, Singh A. Non-echoplanar diffusion weighted imaging in the detection of post-operative middle ear cholesteatoma: navigating beyond the pitfalls to find the pearl. Insights Imaging 2016; 7:669–678. [CrossRef]
10. Kosling S, Bootz F. CT and MR imaging after middle ear surgery. Eur J Radiol 2001; 40:113–118. [CrossRef]
11. Dubrulle F, Souillard R, Chechin D, Vaneecloo FM, Desaulty A, Vincent C. Diffusion-weighted MR imaging sequence in the detection of postoperative recurrent cholesteatoma. Radiology 2006; 238:604–610. [CrossRef]
12. Thiriat S, Riehm S, Kremer S, Martin E, Veillon F. Apparent diffusion coefficient values of middle ear cholesteatoma differ from abscess and cholesteatoma admixed infection. AJNR Am J Neuroradiol 2009; 30:1123–1126. [CrossRef]
13. Mas-Estelles F, Mateos-Fernandez M, Carrascosa-Bisquert B, Facal de Castro F, Puchades-Roman I, Morera-Perez C. Contemporary non-echo-planar diffusion-weighted imaging of middle ear cholesteatomas. Radiographics 2012; 32:1197–1213. [CrossRef]
14. Lingam RK, Khatri P, Hughes J, Singh A. Apparent diffusion coefficients for detection of postoperative middle ear cholesteatoma on non-echo-planar diffusion-weighted images. Radiology 2013; 269:504–510. [CrossRef]
15. Vercruysse JP, De Foer B, Pouillon M, Somers T, Casselman J, Offeciers E. The value of diffusion-weighted MR imaging in the diagnosis of primary acquired and residual cholesteatoma: a surgical verified study of 100 patients. Eur Radiol 2006; 16:1461–1467. [CrossRef]
16. De Foer B. Non echo planar, diffusion-weighted magnetic resonance imaging (periodically rotated overlapping parallel lines with enhanced reconstruction sequence) compared with echo planar imaging for the detection of middle-ear cholesteatoma. J Laryngol Otol 2011; 125:877–878. [CrossRef]
17. De Foer B, Vercruysse JP, Bernaerts A, et al. The value of single-shot turbo spin-echo diffusion-weighted MR imaging in the detection of middle ear cholesteatoma. Neuroradiology 2007; 49:841–848. [CrossRef]
18. Karandikar A, Loke SC, Goh J, Yeo SB, Tan TY. Evaluation of cholesteatoma: our experience with DW Propeller imaging. Acta Radiol 2015; 56:1108–1112. [CrossRef]
19. Kasbekar AV, Scoffings DJ, Kenway B, et al. Non echo planar, diffusion-weighted magnetic resonance imaging (periodically rotated overlapping parallel lines with enhanced reconstruction sequence) compared with echo planar imaging for the detection of middle-ear cholesteatoma. J Laryngol Otol 2011; 125:376–380. [CrossRef]
20. Alsop DC. Phase insensitive preparation of single-shot RARE: application to diffusion imaging in humans. Magn Reson Med 1997; 38:527–533. [CrossRef]
21. Elefante A, Cavaliere M, Russo C, et al. Diffusion weighted MR imaging of primary and recurrent middle ear cholesteatoma: an assessment by readers with different expertise. Biomed Res Int 2015; 2015:597896. [CrossRef]
22. Dhepnorrarat RC, Wood B, Rajan GP. Postoperative non-echo-planar diffusion-weighted magnetic resonance imaging changes after cholesteatoma surgery: implications for cholesteatoma screening. Otol Neurotol 2009; 30:54–58. [CrossRef]
23. Lehmann P, Saliou G, Brochart C, et al. 3T MR imaging of postoperative recurrent middle ear cholesteatomas: value of periodically rotated overlapping parallel lines with enhanced reconstruction diffusion-weighted MR imaging. AJNR Am J Neuroradiol 2009; 30:423–427. [CrossRef]
24. Rajan GP, Ambett R, Wun L, et al. Preliminary outcomes of cholesteatoma screening in children using non-echo-planar diffusion-weighted magnetic resonance imaging. Int J Pediatr Otorhinolaryngol 2010; 74:297–301. [CrossRef]
25. Pizzini FB, Barbieri F, Beltramello A, Alessandrini F, Fiorino F. HASTE diffusion-weighted 3-Tesla magnetic resonance imaging in the diagnosis of primary and relapsing cholesteatoma. Otol Neurotol 2010; 31:596–602. [CrossRef]
26. Akkari M, Gabrillargues J, Saroul N, et al. Contribution of magnetic resonance imaging to the diagnosis of middle ear cholesteatoma: analysis of a series of 97 cases. Eur Ann Otorhinolaryngol Head Neck Dis 2014; 131:153–158. [CrossRef]
27. Cavaliere M, Di Lullo AM, Caruso A, et al. Diffusion-weighted intensity magnetic resonance in the preoperative diagnosis of cholesteatoma. ORL J Otorhinolaryngol Relat Spec 2014; 76:212–221. [CrossRef]
28. Khemani S, Lingam RK, Kalan A, Singh A. The value of non-echo planar HASTE diffusion-weighted MR imaging in the detection, localisation and prediction of extent of postoperative cholesteatoma. Clin Otolaryngol 2011; 36:306–312. [CrossRef]
29. Venail F, Bonafe A, Poirrier V, Mondain M, Uziel A. Comparison of echo-planar diffusion-weighted imaging and delayed post-contrast T1-weighted MR imaging for the detection of residual cholesteatoma. AJNR Am J Neuroradiol 2008; 29:1363–1368. [CrossRef]
30. Nash R, Wong PY, Kalan A, Lingam RK, Singh A. Comparing diffusion weighted MRI in the detection of post-operative middle ear cholesteatoma in children and adults. Int J Pediatr Otorhinolaryngol 2015; 79:2281–2285. [CrossRef]
31. Suzuki H, Sone M, Yoshida T, et al. Numerical assessment of cholesteatoma by signal intensity on non-EP-DWI and ADC maps. Otol Neurotol 2014; 35:1007–1010. [CrossRef]
32. Chou MC, Wang CY, Liu HS, Chung HW, Chen CY. Pseudolesions arising from unfolding artifacts in diffusion imaging with use of parallel acquisition: origin and remedies. AJNR Am J Neuroradiol 2007; 28:1099–1101. [CrossRef]
33. Kolff-Gart AS, Pouwels PJ, Noij DP, et al. Diffusion-weighted imaging of the head and neck in healthy subjects: reproducibility of ADC values in different MRI systems and repeat sessions. AJNR Am J Neuroradiol 2015; 36:384–390. [CrossRef]